

# Structural Insight Into Functional Aspects of Ribosomal RNA Targeting

Ada Yonath\*<sup>[a]</sup>

## 1. Introduction

Ribosomes are giant riboprotein assemblies that play the main role in the translation of the genetic code into proteins. All ribosomes consist of two subunits of unequal size with defined tasks. The small ribosomal subunit is involved in the initiation of the translation process, in choosing the translated frame, in decoding the genetic message, and in controlling the fidelity of codon–anticodon interactions. The large subunit catalyzes the formation of the peptide bond and gates the nascent chains by channeling them through their dynamic exit tunnel.

Messenger RNA (mRNA) and tRNA carry the genetic information and the amino acids, respectively. The ribosome possesses a channel along which the mRNA chain progresses and three tRNA binding sites, designated as A (aminoacyl), P (peptidyl), and E (exit). All tRNA molecules are built primarily of double helices, with an anticodon stem loop at one end and a single-stranded CCA moiety on their other end. The amino acids to be incorporated in the nascent proteins and the newly formed polypeptide chains bind to the CCA end. The mRNA and the anticodon loop of the tRNA molecules interact with the small subunit, whereas the acceptor stem and the 3' end of the tRNA molecules bind to the large subunit. Hence, each of the three tRNA molecules is located on both subunits, which act in concert during the elongation cycle in order to translocate the A- and P-tRNA molecules together with the mRNA by precisely one codon.

Recently obtained crystal structures of ribosomal particles showed unambiguously that both ribosomal active sites, namely the decoding and peptidyl transferase centers, consist exclusively of ribosomal RNA (rRNA). As the primary actor in the process of protein biosynthesis, the ribosomal RNA is targeted by substrates, by nonribosomal factors participating in the process, and by antibiotics and inhibitors. Many clinically relevant antibiotics hamper ribosomal functions by binding primarily to ribosomal RNA. Self-rRNA targeting plays a major role in the creation of functional ribosomes. This article highlights recent advances in studies aimed at the understanding of the molecular mechanisms that are triggered, accomplished, or assisted by rRNA interactions.

## 2. Self-Targeting

Accurate positioning of the two ribosomal subunits relative to each other is the key for the correct assembly of functionally active ribosomes. Since the intersubunit interface is composed mainly of rRNA; the intersubunit bridges formed upon the

association of the two subunits are also composed mainly of rRNA. These bridges contribute significantly not only to the maintenance of the associated ribosome, but also to its various functions, as they possess inherent conformational mobility. There are structural indications that in most cases the small subunit components of the bridges preserve a similar conformation in the bound and unbound states, whereas those originating from the large subunit are inherently flexible.

The intersubunit bridge called B2a is located in the heart of the ribosomal activity region. Its large subunit component, helix H69 of the 23S RNA (numbering according to *E. coli* throughout), is a highly flexible multitask feature.<sup>[1–3]</sup> In the assembled *Thermus thermophilus* ribosome T70S it stretches out towards the small subunit and interacts with both the A-site and the P-site tRNA molecules.<sup>[4]</sup> In the unbound large subunit of *Deinococcus radiodurans* D50S it is positioned on the subunit interface in a distinctly different conformation and interacts with neighboring RNA features<sup>[1]</sup> as well as with A-site tRNA mimics (Figure 1a, b).<sup>[2]</sup> Similar to the large subunit feature of the A-finger bridge which is built of helix H38, H69 is disordered in the structure of the large ribosomal subunit from *Haloarcula marismortui* H50S.<sup>[5]</sup>

It is likely that the ribosome benefits from the flexibility of H69 beyond its participation in intersubunit bridging.<sup>[2, 6, 7]</sup> Helix H69 and its extension, helix H70, originate near the peptidyl transferase center (PTC) in the large subunit, and reach the vicinity of the decoding site in the small subunit. This bridge connects the two ribosomal active sites and seems to be designed for transmitting signals between them. Its proximity to both the A- and the P-site tRNAs in the large subunit suggests that it may also participate in translocation by assisting the shift of the A-site tRNA acceptor stem into the P site. Helix H69 is also one of the constituents of the upper side of PTC that makes crucial contributions to the remote interactions that govern the precise positioning and accurate orientation of the tRNA substrates.<sup>[2, 7]</sup>

[a] Prof. A. Yonath  
Dept. of Structural Biology  
The Weizmann Institute  
76100 Rehovot (Israel)  
and Max-Planck-Research Unit for Ribosomal Structure  
22603 Hamburg (Germany)  
Fax: (+972) 8 934 4154  
E-mail: ada.yonath@weizmann.ac.il

### 3. PTC Targeting

Crystal structures of complexes of T70S with three tRNA molecules and of D50S with substrate analogues mimicking the tRNA acceptor stem revealed that these tRNA helical features interact extensively with the upper side of the PTC pocket.<sup>[2, 4]</sup> Analysis of the binding modes of substrate analogues designed to mimic specific tRNA regions of different sizes allowed the assessment of the relative significance of their interactions with the large ribosomal subunit.<sup>[2, 7]</sup> It was found that remote interactions of the A-site tRNA acceptor stem with the upper side of PTC (Figure 1c) dominate the precise positioning of its

Ada Yonath pioneered ribosomal crystallography and inspired the high-resolution structure determination of the only cellular organelle so far exposed to crystallographic studies. When she initiated ribosomal crystallography, much doubt was expressed. Nevertheless, she demonstrated the feasibility of ribosomal structure determination by pushing crystallography to its limits and by the introduction of flash cryobiocrystallography, an innovative method for minimizing the extreme irradiation sensitivity of biological crystals. This method became instantaneously the state-of-the-art procedure and revolutionized structural biology by enabling researchers to do projects considered impossible. Among Prof. Yonath's unique achievements is the determination of the functionally relevant high-resolution structures of both ribosomal subunits. Since the ribosomal particles crystallized by her were found to be suitable pathogen models, she deciphered the modes of action of over a dozen antibiotics targeting the ribosome, and unraveled the mechanisms of antibiotic selectivity and resistance, thus paving the way for structural-based drug design. Her studies are on ribosomal complexes with substrate analogues, antibiotics, and factors. She deciphered the universal nature of initiation of protein biosynthesis and the step governing the selection of the correct frame to be translated, and revealed the uniform mechanism of peptide-bond formation, translocation, and the direction of nascent proteins into their exit tunnel. This tunnel, detected by Prof. Yonath in the mid-eighties and controversial for almost a decade, was assumed to be the passive path taken by the protein chains. Recently, Prof. Yonath provided the first high-resolution structural basis for the dynamic properties of the tunnel and illuminated its gating and discrimination functions, which indicate that the ribosome is not only a ribozyme translating the genetic code, but is also involved in intracellular regulation processes.

Prof. Yonath is a member of the Israeli and USA National Academies of Sciences. She leads two research groups, at the Max-Planck Research Unit in Hamburg and at the Weizmann Institute, where she directs two scientific centers for structural molecular biology and holds the Martin Kimmel Professorial chair. She is a member of the ChemBioChem Editorial Advisory Board.

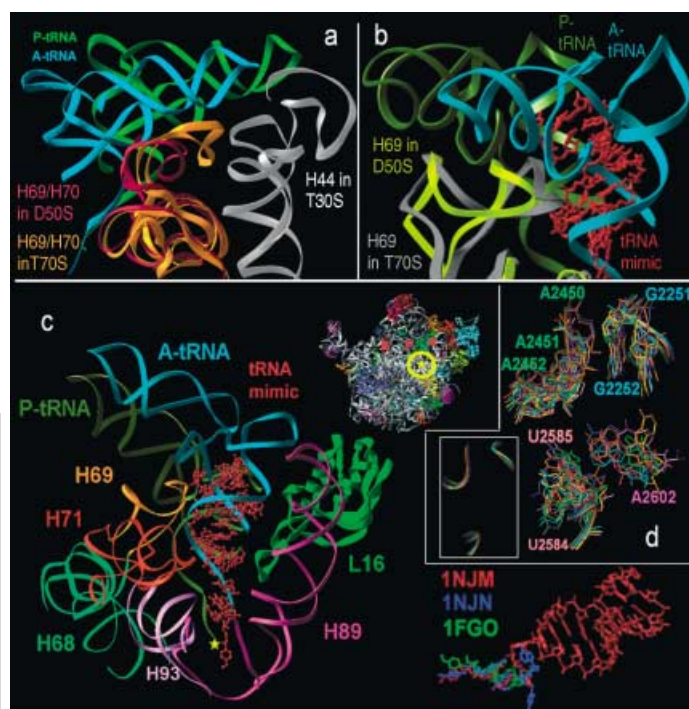


**Figure 1.** Helix H69 and remote substrate positioning in the PTC. The docked A- and P-site tRNAs, based on the structure of the complex of T70S ribosome with three tRNA molecules,<sup>[4]</sup> are shown as ribbons in cyan and olive-green, respectively. The tRNA mimic, made of 35 nucleotides representing the tRNA acceptor stem,<sup>[2]</sup> is shown as red atoms. a) and b) show two views of the two observed conformations of H69 in the assembled T70S<sup>[3, 7]</sup> and in the unbound D50S.<sup>[1]</sup> The suggested stretching-out motion towards the small subunit active site, as evident from (a) and (b), shows how the inherent mobility of helix H69 may provide assistance to the translocation of the tRNA double-helical acceptor stem. c) Left (main figure): The PTC and its vicinity; right (small figure): the intersubunit face of the large subunit D50S. The upper side of PTC interacts intensively with the tRNA acceptor stem and govern the correct placement and orientation of the A-site RNA or its acceptor stem mimics, including the orientation of the tRNA 3' ends in the lower part of the PTC pocket, the site of formation of the peptide bond. The yellow stars (within the PTC and on the intersubunit interface of the large subunit) indicate the approximate location of the site of peptide-bond formation. Right (small figure): A superposition of the locations of two substrate analogues that do not interact with H69 in the upper part of the PTC. One of these, 1NJN, is a short puromycin derivative (ACC-puromycin) bound to D50S.<sup>[2]</sup> The second, 1FGO, is the lower part of an acceptor stem mimic bound to H50S. The double-helical features of this mimic were not detected in the map since no interactions could be made with H69, as this helix is disordered in the H50S structure.<sup>[9]</sup> The various orientations at the active site indicate the PTC tolerance and illustrate the major contributions of the remote interactions for the precise positioning of the ribosomal substrates. d) Superposition of the different conformations of several PTC nucleotides observed in different crystal forms. For comparison, the superposition of the backbones of the same region is shown in the insert. Color code: H50S is shown in purple. Cyan, blue, brown, and yellow are H50S complexes, with Protein data bank accession codes: 1FGO, 1M90, 1FFZ, and 1KQS, respectively. D50S is shown in gray, its complex with the acceptor stem mimic in red, and with the short substrate ACCP in green.

aminoacylated 3' end in the lower end of the PTC, the site of formation of the peptide bond.<sup>[2, 7]</sup> Remote placement of the A-site 3' end of the tRNA seems to be designed to allow variability in PTC binding, which is required to comply with the ability of the ribosome to accommodate all of the amino acids, namely reactants of significantly different chemical structures, sizes, and shapes.

The major contribution of the remote interactions to the correct alignment of the tRNA substrates is demonstrated by the finding that in the absence of these interactions, similar, but distinctly different, PTC–substrate binding modes are formed (Figure 1 c). Lack of remote interactions may be the result of the disorder of H69, as observed in the H50S structure,<sup>[5, 9]</sup> or result from the use of tRNA analogues that are too short to reach the upper side of the PTC,<sup>[2, 9–11]</sup> where the components provide the remote interactions reside.<sup>[2, 7]</sup> Importantly, substrate orientation dictated by remote interactions leads to optimal stereochemistry for the formation of a peptide bond,<sup>[2, 7]</sup> whereas binding independent of remote directionality leads to orientations requiring significant conformational rearrangements to participate in formation of a peptide bond.<sup>[8]</sup>

The ability of the ribosome to bind a large range of compounds, among them partially disordered substrate analogues and compounds considered inaccurately reaction intermediates,<sup>[8, 11]</sup> demonstrates the relative ease of binding of mimics of the 3' end of tRNA. However, the mere binding of such compounds does not imply that each of the bound compounds can participate in protein production without undergoing minor or major conformational rearrangements. The diversity of binding modes observed in the different crystal forms of the large subunit is consistent with the variability in PTC conformations observed in the different crystal forms,<sup>[1, 4]</sup> (Figure 1 d) despite the high sequence conservation in PTC and indicates that the PTC tolerates various orientations. Furthermore it hints at the possible involvement of the PTC in the substrate reorganizations required for the formation of peptide bonds by compounds bound originally in a non- or semiproductive manner. Such conformational rearrangements are bound to consume time, hence rationalizing the relatively low rate of peptide bond formation by short mimics such as puromycin derivatives.<sup>[8]</sup>

### 3.1 Spiral Rotation—The Dynamics of Substrate Targeting

Processivity of protein biosynthesis requires the fast and efficient formation of a peptide bond accompanied by large-scale and modest motions of ribosomal features<sup>[1, 2, 6, 12–14]</sup> that act in concert to facilitate translocation. The immense contribution of the ribosomal template to the correct positioning of the tRNA molecules was discussed above. As argued below, and shown previously,<sup>[2, 7]</sup> it appears that the ribosome also provides the pattern, or the scaffold, for tRNA translocation.

The ribosome is basically an asymmetric particle. Yet, a symmetry-related region (SRR) of a significant size (around 180 nucleotides; Figure 2 a–c), which relates the A- and the P-regions of the PTC was revealed in all known structures of the large ribosomal subunit.<sup>[1, 2, 4, 9–11]</sup> The 3' ends of the A- and the P-site tRNA are two similar chemical moieties that have to face each other to result in the proper stereochemistry of the formed peptide bond. The necessity of offering two comparable supportive environments in the PTC to host these two similar reactants, justifies the existence of a region related by twofold symmetry. The detection of a twofold symmetry even in H50S complexes containing short or partially disordered substrate analogues and inaccurate intermediates,<sup>[9]</sup> both of which require

additional rearrangements to participate in the formation of a peptide bond,<sup>[8, 11]</sup> indicates the importance of the symmetry-related binding in the PTC. Only a few outliers have been detected within this region, among them the very flexible universal nucleotide A2602, the base of which almost coincides with the axis (Figure 2 b, d). As described below, the significance of the internal ribosomal symmetry expands beyond the mere binding of the two 3' ends of the tRNA.

The twofold symmetry axis of the SRR is positioned close to the PTC center, approximately midway between the A and the P loops, and is directed into the tunnel (Figure 2 e). It almost overlaps with the bond connecting the double-helical features of the A-site tRNA with its single-stranded 3' end, the moiety carrying the amino acids. Analysis of the architecture of the PTC by looking down the axis revealed an arched void with a width sufficient to accommodate the 3' ends of the tRNA (Figure 2 c) which appears to be designed to have the exact pattern required for the rotation of the 3' end of the A-site tRNA into the P site. Consequently, the tRNA A- to P-site rotation is likely to involve two independent, albeit correlated, motions: a shift of the A-tRNA helical regions, performed as a part of the overall mRNA/tRNA translocation, and a spiral rotation of the 3' end of the tRNA, which creates favorable stereochemistry for the formation of a peptide bond and seems to be performed in conjunction with it.<sup>[2, 7]</sup>

The remarkable features of this design are the PTC walls. The wall located farthest away from the subunit interface, called the rear wall, forms the scaffold that guides and secures the rotary motion. Two nucleotides of the opposite PTC wall anchor this motion, thus confining the precise path and ensuring that the rotating moiety, together with the aminoacylated A-site tRNA, will have optimal stereochemistry for formation of a peptide bond upon reaching the P site (Figure 2 f). While rotating, the 3' end of the A site slides along the backbone of two rear-wall nucleotides and interacts with several rear-wall bases that point inwards. The two universally conserved nucleotides anchoring the motion from the front side of the PTC, A2602 and U2585, bulge into the PTC center and do not obey the twofold symmetry (Figure 2 c, e). Within the PTC, A2602 is the base that undergoes the largest conformational rearrangements upon substrate or inhibitor binding, and superposition of all of its known conformations revealed that it has a different orientation in each of the known complexes of the large subunit (Figure 2 d). This striking conformational variability is consistent with the unique role of A2602 in the tRNA hydrolysis of the peptidyl-ester bond during termination<sup>[15]</sup> and appears to be synchronized with the rotatory motion. Consequently, we proposed that nucleotide A2602 acts as a conformational switch within the PTC by propelling the rotating moiety (Figure 2 b, d), most likely in concert with the action of helix H69—the feature that seems to assist the shift of the tRNA acceptor stem at the subunit interface.<sup>[3, 6]</sup>

The twofold symmetry relates to the backbone fold and nucleotide orientation rather than to the nucleotide identity (Figure 2 a, b). Thus, despite the substantial conformational variability of the PTC bases,<sup>[1, 3, 4]</sup> the overall symmetry of its backbone is practically preserved in all the known structures

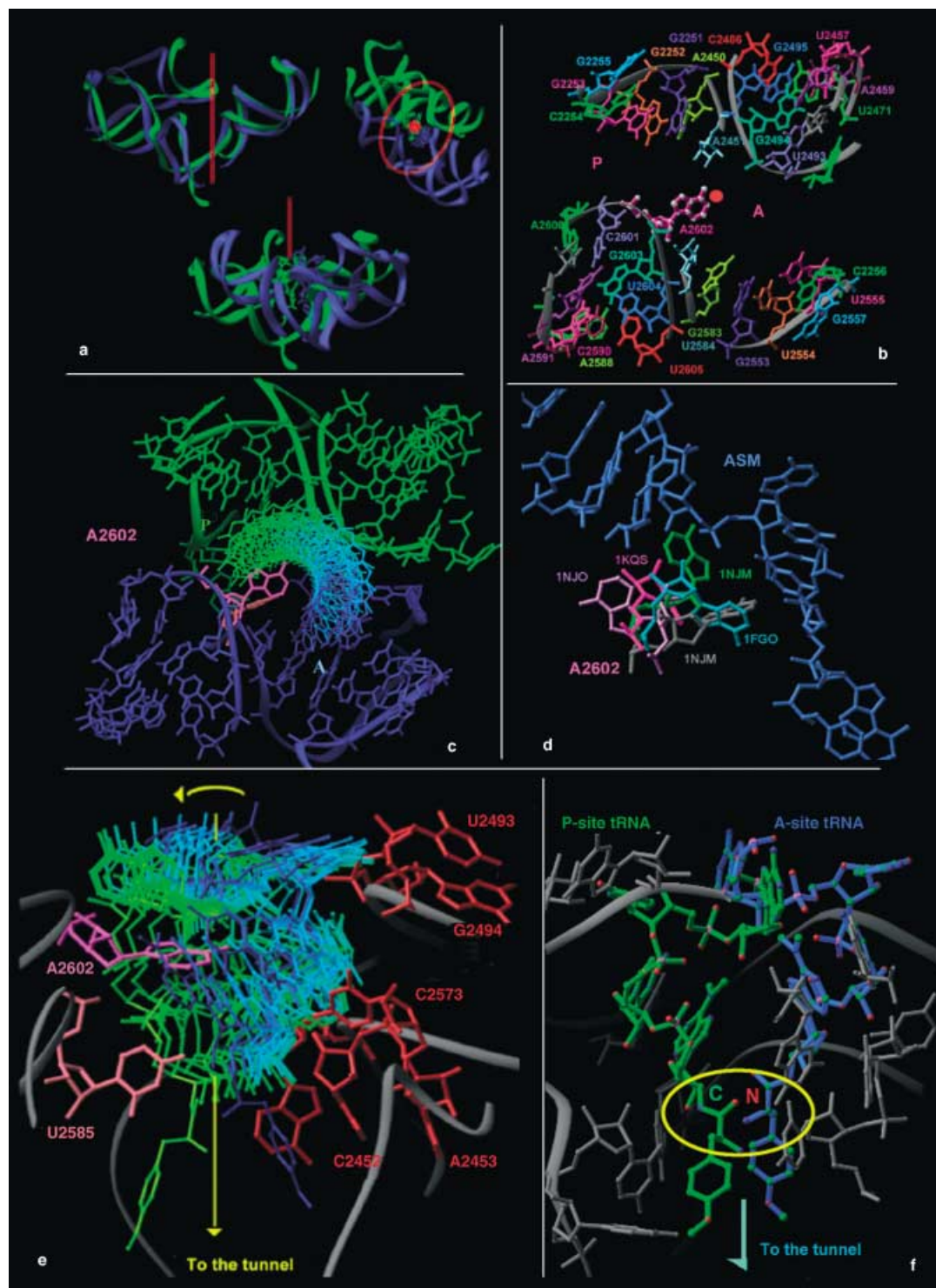


**Figure 2.** The symmetry-related region and the rotatory motion. Except for (b), the symmetry-related regions as well as the observed A-site mimic and the derived P-site are shown in blue and green, respectively. The twofold symmetry axis is shown by red dots or lines. a) Three views of the features related by symmetry. Upper left: superposition of one half of the symmetry related region on its second half. Top right and bottom: perpendicular views of the entire region. The red circle embraces the inner core of the region, at the PTC. A detailed view of this region is given in (b) and (c), each showing a projection down the twofold rotation axis within the core of the symmetry-related region in D50S. In (b) symmetry related nucleotides are colored identically. Note that A2602 is located at the center, very close to the twofold axis. It bulged out of the SRR region and does not obey the twofold symmetry. d) The various orientations, induced by substrate binding, of A2602. The substrates are named by their PDB accession codes. Note the complementarity between the imaginary surface of A2602 orientations and that of the tRNA acceptor stem mimic. c,e) Snapshots of the spiral motion from the A site (blue) to the P site (green), obtained by successive rotations of the rotating moiety by  $15^\circ$  each around the twofold axis. This rotation is represented by the transition from the A-site aminoacylated tRNA (in blue) to the P site (in green). In (c) note the pattern provided by the PTC for the exact A  $\rightarrow$  P rotatory motion. In (e) note that the support and precise guidance seems to be given by the PTC rear-wall nucleotides (in red) and the anchoring of the front nucleotides A2602 (magenta) and U2585 (pink). f) The positions of the acceptor stem A-tRNA mimic and the derived P-site tRNA at the end of the rotatory motion. N is the nucleophilic amine at the A site, and C is the carbonyl carbon atom at the P site.

(Figure 1d). Deviations from the twofold symmetry, detected mainly in bulged nucleotides, seem to be instrumental for specific PTC tasks. One of these is the first rotatory motion, for which the sole geometrical requirement is the binding of the initial aminoacylated tRNA in the P site in the flipped orientation. At this stage both the A and the P site are unoccupied, therefore, the correct selection of the binding site as well as the binding mode by the initiator tRNA is critical. Comparison of potential interactions in the two PTC binding sites showed that, compared to the A site, the P site contains an extra potential interaction which can be exploited by a flipped 3' end of the tRNA, thus indicating the preference for this mode of binding.

The specific locations and orientations of other deviations from the twofold symmetry indicate their feasible contribution to the inherent chirality of the proteins, to the irreversible entrance of the nascent proteins into the tunnel (with the lower P-site nucleotides residing at the entrance to the tunnel), to translocation (for example, molecular switches), and for preserving productive PTC conformations. An intriguing example of the latter task is the bulged out nucleotide G2250 in the P site that interacts with the flexible loop of protein L16, the only protein that is involved in the remote positioning of the A-site tRNA. It is conceivable that its interaction with G2250 stabilizes the favorable conformation of L16 loop, thus hinting at an interplay between the P and the A sites within the PTC. Importantly, among the nucleotides composing the P site, four are located somewhat deeper in the PTC compared to the situation at the A site, which implies there is a modest spiral nature to the twofold axis.<sup>[2, 7]</sup> The outcome of this spiral motion is that a P-site carbonyl carbon atom faces the A-site nucleophilic amine, and a newly created peptidyl points into the tunnel.

The 3' end of the correctly placed aminoacylated tRNA enables it to flip into the P site without any significant conformational alterations. Indeed, the entire rotatory motion could be simulated without any steric hindrances or space constraints. Importantly, the interactions of the PTC with both the A-site tRNA and the derived P-site tRNA are consistent with most of the available biochemical, cross-linking, and footprinting data.<sup>[16–18]</sup> In contrast, simulation studies showed that all substrate analogues that were not positioned by remote interaction<sup>[2, 9–11]</sup> could not be rotated through the curved PTC rotatory motion pattern without clashes with its walls.<sup>[2, 7]</sup>

We have previously suggested that the spiral rotatory motion is the key component of unified ribosomal mechanism for peptide-bond formation, translocation, and nascent protein progression.<sup>[2, 7]</sup> This integrated ribosomal machinery indicates spontaneous formation of a peptide bond concurrent with the movement of the A-tRNA acceptor stem into the P site,<sup>[18]</sup> and is consistent with the suggestion that the main task of the ribosome in catalyzing peptidyl transferase activity is the provision of the framework for precise positioning of the tRNA molecules.<sup>[1, 2, 7, 19–21]</sup> Noteworthy is the SRR architecture: it consists of three semicircular shells, positioned between the two lateral protuberances of the large ribosomal subunit.<sup>[7]</sup> Only 17 out of the 90 nucleotide couples of the SRR belong to its inner core (Figure 2a, b) and these reside within the PTC or in its immediate neighborhood. The extension of the SRR beyond the

PTC seems to play a role in amplifying the stabilization of its functional core and may be linked to signaling between the incoming and leaving tRNA molecules.<sup>[7]</sup>

The detection of similar symmetry-related regions in all known structures of the large subunit, the high conservation of most of the nucleotides belonging to it, the pattern designed for the spiral rotation, the ensured entrance of the nascent proteins into the ribosomal exit tunnel, the possible mediation of signals between functionally relevant remote locations, and the resulting stereochemistry suitable for peptide-bond formation are consistent with the universality of the proposed unified mechanism.

### 3.2 Targeted Peptide-Bond Formation

The guidance provided by the PTC to the rotatory moiety positions it into an orientation and at a distance suitable for peptide-bond formation. Thus, at the end of the spiral rotation, the carbonyl carbon atom of the peptidyl tRNA is positioned in a stereochemistry suitable for nucleophilic attack by the A-site primary amine of the aminoacylated tRNA (Figure 2f). This attack should readily occur at the pH value (7.8–8) within the D50S crystals,<sup>[1]</sup> which is an optimal pH value for protein biosynthesis in almost all species, including *E. coli* and *H. marismortui*.<sup>[16, 22–26]</sup> Nucleophilic attack generates a tetrahedral oxyanion intermediate, which is followed by SP2 → SP3 reorganization and a transfer of a hydrogen atom to the leaving group. The simultaneous rotatory motion results in the entrance of the 3' end of the A-site tRNA into the P site, thus guaranteeing the release of the P-site leaving group and ensuring the processivity of protein biosynthesis. According to this mechanism, no PTC ribosomal components are required during the entire process for the actual chemical events associated with formation of a peptide bond. They do provide, however, an elaborate framework for accurate substrate positioning and for smooth substrate motions. Nevertheless, selected PTC components may play a critical role in the stabilization of reaction intermediates. They may also contribute to cell vitality by influencing the reaction rate.<sup>[27]</sup>

Apart from GTPase hydrolysis, peptide-bond formation is considered to be a fast reaction compared to other steps of protein biosynthesis.<sup>[28]</sup> This step seems to carry the entire protein biosynthesis process forward, including codon–anticodon recognition in the small subunit, the GTPase activation, and accommodation of the the A-site tRNA in the large subunit. It is conceivable, therefore, that the degenerate framework resulting from the twofold symmetry has a central dynamic role. Once the incoming tRNA is positioned in the PTC in a favorable conformation, which is dictated by this framework, it only has to rotate into the second part of the framework. Saving reorganization time is crucial for fast reaction rates and may enable conversion of the equilibrium of the chemical reaction to proceed toward formation of a peptide bond. An additional benefit of the twofold symmetry is the alternating directions of the side chains incorporated into the nascent peptide that should minimize steric hindrances.

The location of the PTC in a protein-free environment;<sup>[1, 2, 5, 9]</sup> the experiments showing that the ribosomal RNA has peptidyl transferase activity;<sup>[24]</sup> and the immense knowledge of mechanisms of enzymatic catalysis led to a hypothesis that the ribosome catalyzes the formation of a peptide bond by a mechanism resembling the reverse mode of action of serine proteases.<sup>[9]</sup> This hypothesis was based on the crystal structure of H50S and of its complexes with either a partially disordered tRNA mimic or a compound presumed to resemble a reaction intermediate,<sup>[9]</sup> but this was shown later to present an inaccurate picture of this state.<sup>[8, 11]</sup> According to this hypothesis specific PTC nucleotides participate in the actual nucleophilic attack and provide stabilization of the oxyanion intermediate.

Evidence obtained from a battery of functional, biochemical, and mutational experiments led to considerable doubt.<sup>[21, 25, 29, 30]</sup> The uncertainties concerning the proposed mechanism were later verified by crystallographic analyses of additional structures of complexes of the same ribosomal subunit, H50S. Although the later experiments were performed under conditions almost identical to those of the original studies, they yielded radically different results. Thus, A2451, the base originally suggested to be the main player in the proposed mechanism, was found to point away from the proposed location of the oxyanion intermediate,<sup>[8, 11]</sup> and is thus unlikely to perform its originally assigned tasks. Moreover, these results show unambiguously that the catalytic role of the ribosome is the precise alignment of the reactants,<sup>[8]</sup> and that there is no ground for the expectation that a common enzymatic mechanism for the hydrolysis of the peptide bond will resemble its intricate and complicated synthesis.

Remarkably, five different H50S complexes<sup>[8, 9–11, 31]</sup> were needed to substantiate the conclusion evident by mere inspection of the D50S structure,<sup>[1]</sup> which was later verified by a single functional complex.<sup>[2]</sup> Importantly, the D50S complexes differ from all of the H50S complexes in that helix H69 is fully ordered in the D50S crystals,<sup>[1]</sup> and thus can provide the remote interactions vital for correct substrate positioning,<sup>[2]</sup> which is in contrast to the disorder seen in the H50S structure.<sup>[5]</sup> The inherent discrepancies between the various modes of substrate positioning in H50S crystals and the finding that all of the binding modes observed in H50S complexes require conformational arrangements, question the functional relevance of H50S crystals and their likelihood to lead to the elucidation of the mechanism of peptide-bond formation. It has been argued that compounds different from those used originally will present more accurate pictures of the reaction.<sup>[8]</sup> However, the finding that all substrate analogues, even that which mimicks the tRNA acceptor stem and is similar to the compound used in D50S studies,<sup>[2]</sup> bind to H50S but that all require conformational rearrangement to obtain a proper peptide-bond stereochemistry<sup>[8]</sup> challenge these expectations.

It is conceivable that the mode of analogue binding is influenced by the functional state of the crystalline H50S particles. Correlation between the ribosomal functional state and the conformation of its PTC has been suggested on the basis of biochemical evidence.<sup>[22]</sup> Similarly, the disorder of almost all of the functionally relevant features in the H50S crystal structure<sup>[5]</sup>

could be correlated to the deviations in the environment within the H50S crystals from the conditions required for efficient protein biosynthesis. Thus, not only is the concentration of the salts about half of the required concentration for high functional productivity, but the pH value is also far from the optimum for protein synthesis.<sup>[8]</sup>

The results of a fragment reaction performed within the H50S crystals support the concern about the suitability of H50S. This reaction led to the dipeptide product CCA-puromycin-phenylalanine-caproic acid-biotin, which did not pass to the P site,<sup>[10]</sup> thus suggesting that the A- → P-site rotation follows formation of the peptide bond. Such a sequence of events is bound to be impractical since it implies considerable conformational rearrangements of the nascent chain within the rather narrow exit tunnel of the protein, which is extremely costly energetically and exceedingly space consuming. Thus, each time a peptide bond is formed, the nascent polypeptide chain has either to rotate by 180° or to compensate for such a twofold rotation by conformational changes of individual main chain bonds of the protein, a necessity that rules out the incorporation of rigid or bulky amino acids, such as proline, histidine, and tryptophane. The formation of a dipeptide within the H50S crystals that stayed at the A site instead of passing to the P site indicates that the formation of a single bond may or may not represent the mechanisms involved in the creation of proteins, and further demonstrated the ability of the PTC to tolerate situations that may not lead to the production of a polypeptide chain.

## 4. Destructive rRNA Targeting

Antibiotics are natural or man-made compounds that are designed to interfere with bacterial metabolism or eliminate bacteria by inhibiting fundamental cell processes. As a central element of the cell cycle, the ribosome is one of the main targets for a broad range of structurally diverse antibiotics that efficiently inhibit different ribosomal functions. The binding sites of over a dozen antibiotics in the large ribosomal subunit were located unambiguously by determining the structures of their complexes with D50S. It was found that all of the antibiotics interact almost exclusively with the rRNA, and although the ribosome theoretically offers multiple opportunities for the binding of these small compounds, practically all of the known drugs utilize only a single or only a few sites.

### 4.1 Inhibitory PTC Targeting

Several clinically relevant antibiotics exert their effects by direct interactions with the PTC. These include chloramphenicol, which interferes with A-site tRNA binding by occupying the position of the amino acid attached to it, and the lincosamide clindamycin, which interacts with both the A and the P site within the PTC, thus preventing peptide-bond formation.<sup>[32]</sup>

Puromycin and sparsomycin are universal inhibitors of protein biosynthesis that were found to be extremely valuable for the understanding of the mechanism of protein biosynthesis, although they have almost no therapeutic relevance. Puromycin targets the PTC A site since its structure resembles the

3' terminus of aminoacyl-tRNA. In the presence of an active donor substrate puromycin can form a peptide bond,<sup>[33]</sup> and hence it is commonly used in functional studies. It is the substrate of choice for the fragment reaction, and its derivatives have been exploited in most of the crystallographic studies described above.

Sparsomycin has a high activity on all cell types, but despite its universality, the binding affinities of sparsomycin differ in different kingdoms.<sup>[34]</sup> Although sparsomycin does not competitively inhibit substrate binding to the A site, A-site inhibitors, such as chloramphenicol, compete with it for binding to bacterial ribosomes.<sup>[35, 36]</sup> Analysis of the structure of sparsomycin complexed with D50S showed that it forms stacking interactions with the base of A2602 which is consistent with previous biochemical results.<sup>[37]</sup> It inhibits peptidyl transferase activity by altering the conformations of both the A and the P loops, thus rationalizing previous controversies. Its dramatic influence on the PTC conformation is a result of its binding to the highly conserved base A2602, a nucleotide that possesses exceptional mobility and is strategically located between the A and the P sites in the PTC (Figure 2 b–d).<sup>[2]</sup>

#### 4.2 Targeting the Ribosomal Tunnel

Once produced, the nascent proteins emerge out of ribosomes through the tunnel adjacent to the PTC. This tunnel is the preferred target of a large number of antimicrobial drugs from the macrolide family, which ranks as the highest in clinical usage. All of the macrolides studied so far bind close to the entrance of the ribosomal exit tunnel, at a distance from the PTC that permits the formation of a polypeptide chain of 5–6 amino acids before reaching the drug. All macrolides block the exit tunnel, but their binding modes, their exact positions, and their precise inhibitory mechanisms may vary significantly.<sup>[32, 38–41]</sup>

All macrolides possess a central lactone ring which is built of 12–22 atoms to which at least one sugar moiety, called desosamine, is bound (Figure 3a). Erythromycin, the “father” of the macrolide family, as well as clarithromycin and roxithromycin, which are improved versions of erythromycin designed to gain stability in acid environments and to have a broad spectrum of activity, bind to the tunnel in a similar way.<sup>[32, 39]</sup>

All three have a 14-membered lactone ring and all interact exclusively with the ribosomal rRNA. The crystallographically observed interactions of the macrolides desosamine sugar with nucleotide A2058 (Figure 3a) are consistent with their biochemical assignment as the key determinant for the binding of 14-membered-ring macrolides.<sup>[42]</sup> The observed interactions of A2058 with the macrolides clarify the mechanism of clinical pathogens acquiring drug resistance by A → G substitution or by the methylation of A2058.<sup>[43]</sup> These interactions also clarify why the replacement of the common prokaryotic adenine by guanine, the typical eukaryotic moiety in this position, acquires selectivity to 14-membered macrolides.

The 15 and 16-membered-ring macrolides bind, under special conditions, to ribosomes with guanine in position 2058. H50S possesses a guanine residue in position 2058, hence, in this critical aspect, the archaeon *H. marismortui* resembles eukar-

yotes more than prokaryotes. By soaking H50S crystals in solutions containing extremely high concentrations of antibiotics, a few macrolides belonging to the 15- and 16-membered-ring macrolide families could be bound to them.<sup>[44]</sup> However, the binding mode of azithromycin to the archaeal H50S differs significantly from that observed for its binding to the eubacterial D50S.<sup>[38]</sup> In D50S, azithromycin lies almost perpendicular to the long axis of the tunnel and almost completely blocks it, similar to all other D50S complexes of clinically relevant macrolides, ketolides, and azalides so far studied.<sup>[32, 38, 40, 41]</sup> In H50S, however, the azithromycin-binding mode leaves a relatively large unoccupied space within the tunnel (Figure 3b), thus justifying the usage of this drug for treating mammals possessing guanine in position 2058.

The superior ability of bacteria to rapidly acquire antibiotic resistance has become a major handicap in modern medicine and stimulated the search for improved drugs. The recently developed ketolides and the azalides have improved pharmacokinetics and enhanced activity against certain macrolide-resistant pathogens. The binding modes of representatives of this group, observed in D50S crystals, show that these newly developed drugs are capable of creating intensive contacts with additional RNA components, and it was suggested that these interactions may compensate for the loss of the contacts with position 2058 (Figure 3a, c). Various mechanisms for enhancing the binding of these antibiotics were observed. Azithromycin binds cooperatively to two sites within the exit tunnel, and the ketolides ABT-773 and telithromycin reach the other side of the tunnel wall, thus contacting RNA features positioned at a large sequence distance.<sup>[38, 40]</sup>

An outstanding binding mode has been observed for troleandomycin (TAO), a semisynthetic derivative of erythromycin that has a modest clinical relevance because of the toxicity of its metabolites. All the moieties capable of participating in hydrogen bonding in TAO are either methylated or acetylated. Nevertheless, it binds close to the tunnel entrance and exploits the binding site favored by macrolides, the vicinity of A2058, albeit by making different contacts (Figure 3d).<sup>[41]</sup> Compared to erythromycin, TAO binds somewhat deeper in the tunnel and its lactone ring is almost parallel to the tunnel wall. In contrast to other macrolides that interact exclusively with the rRNA, TAO interacts with the ribosomal protein L32 and causes cross-tunnel swinging of the entire tip of the beta-hairpin of protein L22 (Figure 3d, e).<sup>[41]</sup> Protein L22 has an intrinsic elongated shape<sup>[45]</sup> and it lines the tunnel wall, extending from the tunnel entrance to the vicinity of its opening (Figure 3e).

The ribosomal exit tunnel, detected first in the 1980s,<sup>[46, 47]</sup> was assumed to be a passive path for nascent proteins.<sup>[9]</sup> However, structural insight into the involvement of ribosomes in the regulation of intracellular co-translational processes was provided recently by crystallographic studies that revealed the conformational mobility of the tunnel.<sup>[41]</sup> Importantly, the crystallographically observed alterations in the conformations of the tunnel could be correlated not only with the structures of antibiotic-resistant mutations,<sup>[48, 49]</sup> but also with tunnel participation in gating and sequence discrimination.<sup>[50–57]</sup> Examples are the secretion monitor (secM) protein<sup>[53, 55]</sup> and the leader peptide

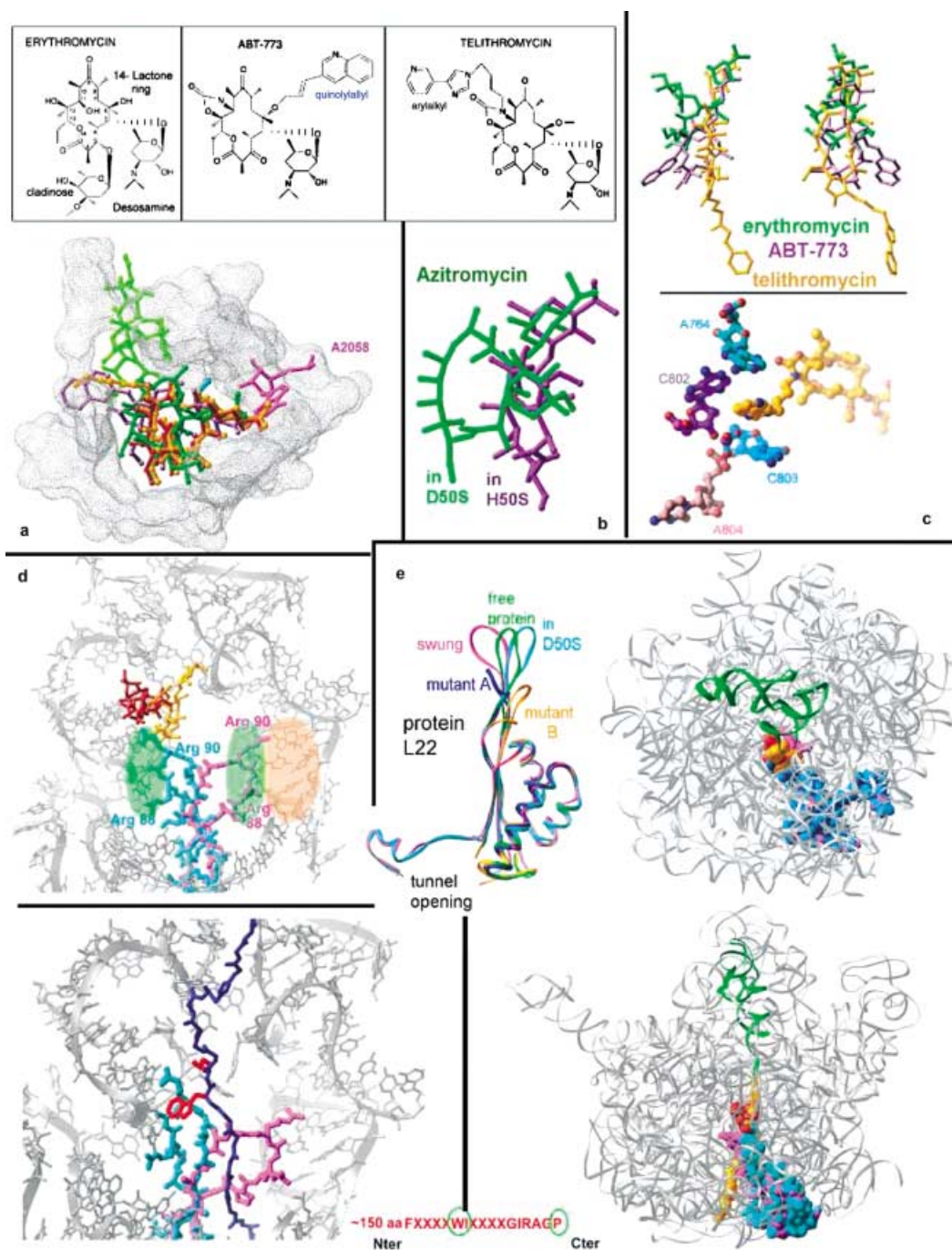


**Figure 3.** Antibiotic action and tunnel gating. D50S RNA is shown as gray ribbons. The tip of the beta-hairpin of protein L22 at its native conformation is shown in cyan, and the swung conformation in magenta. The insert shows the chemical formulas of erythromycin, ABT 773, and telithromycin. a) A view into the tunnel, with the structures of several macrolides and ketolides superimposed on each other, each colored differently. Base 2508 is highlighted in magenta. b) Superposition of the binding modes of azithromycin to H50S<sup>[44]</sup> and to D50S.<sup>[38]</sup> c) The binding modes of two ketolides showing their interactions with additional sites compared to the macrolides, thus explaining their action on several macrolide resistant strains. d) Top: A view along the tunnel showing the positions of erythromycin and TAO and the locations of the L22 hairpin tip in its native and swung conformations. The pink and the green patches indicate protein and RNA regions where mutations relieving arrest were localized.<sup>[55]</sup> Bottom: The same view but with a modeled polypeptide chain in extended conformation<sup>[41]</sup> (shown in blue), with the crucial tryptophane highlighted in red. The entire arrest sequence is given below. e) The location of protein L22 within the large ribosomal subunit from the top of the tunnel and along its side. P-site tRNA is shown in green. All known conformations of protein L22 are superposed in the middle, including the free protein<sup>[45]</sup> and its erythromycin resistant mutant.<sup>[57]</sup> Note the similarity of these structures, except for at the tip of the hairpin region.

of *E. coli* tryptophanase (tnaC) operon.<sup>[56]</sup> The secM protein, produced in conjunction with a protein export system that recognizes an export signal, includes a sequence motif that

causes elongation arrest in the absence of the protein export system. This sequence is located about 150 residues away from the protein N terminus, and within it, separated by 12 residues,



are the main features that trigger elongation arrest: a proline and a tryptophane residue (Figure 3 d, e). Specific mutations in ribosomal protein L22 and in the regions involved in tunnel-wall interactions of the swung conformation of the hairpin tip of L22, similar to those conferring resistance to erythromycin,<sup>[49]</sup> were shown to by-pass the elongation arrest.<sup>[55]</sup> We therefore suggested that a similar swing of the hairpin tip of L22 is exploited for tunnel gating, and that protein L22 together with the already-formed portion of the nascent chain are involved in transmitting signals from the environment into the ribosomal core.<sup>[41]</sup>

## 5. Conclusions

Comparative analysis of the crystal structures of ribosomal particles revealed a sizable symmetry-related region with a stunning architectural design within the otherwise asymmetric ribosome. A unified machinery that integrates peptide-bond formation, translocation, and nascent protein progression was proposed based on the observed remote interactions that govern the precise positioning of the tRNA molecules; on the overlap of the symmetry rotation axis identified in the middle of the PTC with the bond connecting the single-stranded 3' end of tRNA with its acceptor stem; on the arched void in PTC that forms a scaffold guiding the A- to the P-site motion between the tRNA rotating moiety and the PTC rear wall.

According to this unified machinery, PTC structural elements guide the A → P motion of the 3' end of the tRNA by a spiral rotatory motion, which leads to an optimal stereochemistry for formation of a peptide bond and thus enabling the creation of the peptide bonds in conjunction with it. An important component of the unified machinery is the spiral nature of the rotatory motion, which ensures the entrance of newly formed polypeptides into the exit tunnel.

This unified machinery implies that the main catalytic contributions of the ribosome are the provision of an elaborate framework for the alignment of the tRNA molecules at an orientation allowing for spontaneous creation of the peptide bond and the provision of the exact path, thus guiding the translocation of the 3' end of tRNA. The identification of a twofold symmetry in all the known structures of the large subunit, the high conservation of most nucleotides belonging to the inner symmetry related region, the ensured entrance of nascent proteins into the ribosomal exit tunnel, the possible mediation of signal transmissions between the incoming and the leaving tRNA molecules, and the creation of orientation suitable for peptide-bond formation indicate the universality of this unified machinery.

## Acknowledgements

Thanks are due to J.-M. Lehn, M. Lahav, H. Gilon, and R. Berisio for critical discussions; as well as to all members of the ribosome research groups at the Max-Planck Society and the Weizmann Institute for their significant contributions to different stages of this work, with special appreciation to the thoughts and efforts of I.

Agmon, A. Bashan, and M. Kessler. X-ray diffraction data were collected at ID19/SBC/APS/ANL and ID14/ESRF-EMBL. The Max-Planck Society, the Kimmelman Center for Macromolecular Assemblies, the US National Institutes of Health (GM34360), and the German Ministry for Science & Technology (BMBF05-641EA) provided support. A.Y. holds the Helen and Martin Kimmel Professorial Chair.

**Keywords:** antibiotics · exit tunnel · peptide bond formation · ribosomes · RNA

- [1] J. Harms, F. Schluenzen, R. Zarivach, A. Bashan, S. Gat, I. Agmon, H. Bartels, F. Franceschi, A. Yonath, *Cell* **2001**, *107*, 679.
- [2] A. Bashan, I. Agmon, R. Zarivach, F. Schluenzen, J. Harms, R. Berisio, H. Bartels, F. Franceschi, T. Auerbach, H. A. Hansen, E. Kossoy, M. Kessler, A. Yonath, *Mol. Cell* **2003**, *11*, 91.
- [3] A. Yonath, *Annu. Rev. Biophys. Biomol. Struct.* **2002**, *31*, 257.
- [4] M. M. Yusupov, G. Z. Yusupova, A. Baucom, K. Lieberman, T. N. Earnest, J. H. Cate, H. F. Noller, *Science* **2001**, *292*, 883.
- [5] N. Ban, P. Nissen, J. Hansen, P. B. Moore, T. A. Steitz, *Science* **2000**, *289*, 905.
- [6] M. Gluehmann, R. Zarivach, A. Bashan, J. Harms, F. Schluenzen, H. Bartels, I. Agmon, G. Rosenblum, M. Pioletti, T. Auerbach, H. Avila, H. A. Hansen, F. Franceschi, A. Yonath, *Methods*, **2001**, *25*, 292.
- [7] I. Agmon, T. Auerbach, D. Baram, H. Bartels, A. Bashan, R. Berisio, P. Fucini, H. A. Hansen, J. Harms, M. Kessler, M. Peretz, F. Schluenzen, A. Yonath, R. Zarivach, *Eur. J. Biochem.* **2003**, *270*, 2543.
- [8] P. B. Moore, T. A. Steitz, *RNA* **2003**, *9*, 155.
- [9] P. Nissen, J. Hansen, N. Ban, P. B. Moore, T. A. Steitz, *Science* **2000**, *289*, 920.
- [10] T. M. Schmeing, A. C. Seila, J. L. Hansen, B. Freeborn, J. K. Soukup, S. A. Scaringe, S. A. Strobel, P. B. Moore, T. A. Steitz, *Nat. Struct. Biol.* **2002**, *9*, 225.
- [11] J. L. Hansen, T. M. Schmeing, P. B. Moore, T. A. Steitz, *Proc. Natl. Acad. Sci. USA* **2002**, *16*, 16.
- [12] M. S. VanLoock, R. K. Agrawal, I. S. Gabashvili, L. Qi, J. Frank, S. Harvey, *J. Mol. Biol.* **2000**, *304*, 507.
- [13] J. M. Ogle, F. V. Murphy, M. J. Tarry, V. Ramakrishnan, *Cell* **2002**, *111*, 721.
- [14] V. Ramakrishnan, *Cell* **2002**, *108*, 557.
- [15] N. Polacek, M. J. Gomez, K. Ito, L. Xiong, Y. Nakamura, A. Mankin, *Mol. Cell* **2003**, *11*, 103.
- [16] D. Moazed, H. F. Noller, *Nature* **1989**, *342*, 142.
- [17] R. Green, H. F. Noller, *Annu. Rev. Biochem.* **1997**, *66*, 679.
- [18] K. S. Wilson, H. F. Noller, *Cell* **1998**, *92*, 337.
- [19] K. H. Nierhaus, H. Schulze, B. S. Cooperman, *Biochem. Int.* **1980**, *1*, 185.
- [20] T. Pape, W. Wintermeyer, M. Rodnina, *Embo. J.* **1999**, *18*, 3800.
- [21] N. Polacek, M. Gaynor, A. Yassin, A. S. Mankin, *Nature* **2001**, *411*, 498.
- [22] R. Miskin, A. Zamir, D. Elson, *Biochem. Biophys. Res. Commun.* **1968**, *33*, 551.
- [23] A. Shevack, H. S. Gewitz, B. Hennemann, A. Yonath, H. G. Wittmann, *FEBS Lett.* **1985**, *184*, 68.
- [24] H. F. Noller, V. Hoffarth, L. Zimniak, *Science* **1992**, *256*, 1416.
- [25] M. A. Bayfield, A. E. Dahlberg, U. Schulmeister, S. Dorner, A. Barta, *Proc. Natl. Acad. Sci. USA* **2001**, *98*, 10096.
- [26] C. Rodriguez-Fonseca, H. Phan, K. S. Long, B. T. Porse, S. V. Kirillov, R. Amils, R. A. Garrett, *RNA* **2000**, *6*, 744.
- [27] V. I. Katunin, G. W. Muth, S. A. Strobel, W. Wintermeyer, M. V. Rodnina, *Mol. Cell* **2002**, *10*, 339.
- [28] M. V. Rodnina, W. Wintermeyer, *Trends Biochem. Sci.* **2001**, *26*, 124.
- [29] A. Barta, S. Dorner, N. Polacek, *Science* **2001**, *291*, 203.
- [30] J. Thompson, D. F. Kim, M. O'Connor, K. R. Lieberman, M. A. Bayfield, S. T. Gregory, R. Green, H. F. Noller, A. E. Dahlberg, *Proc. Natl. Acad. Sci. USA* **2001**, *98*, 9002.
- [31] P. B. Moore, T. A. Steitz, *Nature* **2002**, *418*, 229.
- [32] F. Schluenzen, R. Zarivach, J. Harms, A. Bashan, A. Tocilj, R. Albrecht, A. Yonath, F. Franceschi, *Nature* **2001**, *413*, 814.
- [33] O. W. Odom, W. D. Picking, B. Hardesty, *Biochemistry* **1990**, *29*, 10734.
- [34] E. Lazaro, L. A. van den Broek, A. San Felix, H. C. Ottenheim, J. P. Ballesta, *Biochemistry* **1991**, *30*, 9642.

- [35] E. Lazaro, C. Rodriguez-Fonseca, B. Porse, D. Urena, R. A. Garrett, J. P. Ballesta, *J. Mol. Biol.* **1996**, *261*, 231.
- [36] G. T. Tan, A. DeBlasio, A. S. Mankin, *J. Mol. Biol.* **1996**, *261*, 222.
- [37] B. T. Porse, S. V. Kirillov, M. J. Awayez, H. C. Ottenheim, R. A. Garrett, *Proc. Natl. Acad. Sci. USA* **1999**, *96*, 9003.
- [38] F. Schluenzen, J. M. Harms, F. Franceschi, H. A. Hansen, H. Bartels, R. Zarivach, A. Yonath, *Structure* **2003**, *11*, 329.
- [39] T. Auerbach, A. Bashan, J. Harms, F. Schluenzen, R. Zarivach, H. Bartels, I. Agmon, M. Kessler, M. Pioletti, F. Franceschi, A. Yonath, *Curr. Drug Targets Infect. Disord.* **2002**, *2*, 169.
- [40] R. Berisio, J. Harms, F. Schluenzen, R. Zarivach, H. A. S. Hansen, P. Fucini, A. Yonath, *J. Bacteriol.* **2003**, *185*, 4276.
- [41] R. Berisio, F. Schluenzen, J. Harms, A. Bashan, T. Auerbach, D. Baram, A. Yonath, *Nat. Struct. Biol.* **2003**, *10*, 366.
- [42] B. Weisblum, *Antimicrob. Agents Chemother.* **1995**, *39*, 577.
- [43] S. Douthwaite, L. H. Hansen, P. Mauvais, *Mol. Microbiol.* **2000**, *36*, 183.
- [44] J. L. Hansen, J. A. Ippolito, N. Ban, P. Nissen, P. B. Moore, T. A. Steitz, *Mol. Cell* **2002**, *10*, 117.
- [45] J. Unge, A. Aberg, S. Al-Kharadaghi, A. Nikulin, S. Nikonov, N. L. Davydova, N. Nevskaya, M. Garber, A. Liljas, *Structure* **1998**, *6*, 1577.
- [46] R. A. Milligan, P. N. Unwin, *Nature* **1986**, *319*, 693.
- [47] A. Yonath, K. R. Leonard, H. G. Wittmann, *Science* **1987**, *236*, 813.
- [48] I. S. Gabashvili, S. T. Gregory, M. Valle, R. Grassucci, M. Worbs, M. C. Wahl, A. E. Dahlberg, J. Frank, *Mol. Cell* **2001**, *8*, 181.
- [49] N. Davydova, V. Streltsov, M. Wilce, A. Liljas, M. Garber, *J. Mol. Biol.* **2002**, *322*, 635.
- [50] S. Liao, J. Lin, H. Do, A. E. Johnson, *Cell* **1997**, *90*, 31.
- [51] R. M. Stroud, P. Walter, *Curr. Opin. Struct. Biol.* **1999**, *9*, 754.
- [52] D. R. Morris, A. P. Geballe, *Mol. Cell Biol.* **2000**, *20*, 8635.
- [53] S. Sarker, K. E. Rudd, D. Oliver, *J. Bacteriol.* **2000**, *182*, 5592.
- [54] T. Tenson, M. Ehrenberg, *Cell* **2002**, *108*, 591.
- [55] H. Nakatogawa, K. Ito, *Cell* **2002**, *108*, 629.
- [56] F. Gong, C. Yanofsky, *Science* **2002**, *297*, 1864.
- [57] S. Jenni, N. Ban, *Curr. Opin. Struct. Biol.* **2003**, *13*, 212.

---

Received: June 11, 2003 [M683]